ETH zürich

Seismic source inversion using Hamiltonian Monte Carlo and a 3-D Earth model for the Japanese Islands

Saulė Simutė [1,2], Lion Krischer [1], Christian Böhm [1], Martin Vallée [2], and Andreas Fichtner [1]

[1] Seismology and Wave Physics Group, ETHZ
[2] Institut de Physique du Globe de Paris, IPGP
saule.simute@erdw.ethz.ch

EGU General Assembly 2020

Short summary of the presentation

Here I present source inversion results for the Japanese Islands. The cool part about this work is that we account for the 3-D heterogeneities of the Earth when computing Green's strains.

To achieve that, we construct a structural model (slides 5 – 6), compute Green's strains for a source area of interest (slides 7 – 8), and perform the inversion using Hamiltonian Monte Carlo (slide 10).

Our results suggest, that properly taking into account the complexity of the medium at shorter periods (15 s) allows for a larger double-couple (DC) component. In turn, large compensated linear vector dipole (CLVD) component appears to be caused by incorrect Green's functions (slides 11 – 14).

Motivation

Green's functions for the same source-receiver path computed for 1-D (top) and 3-D (bottom) models clearly differ. If we were to use these 1-D Green's functions in the source inversion – all of this waveform difference would be incorrectly attributed to the source, while it is actually a structural effect.

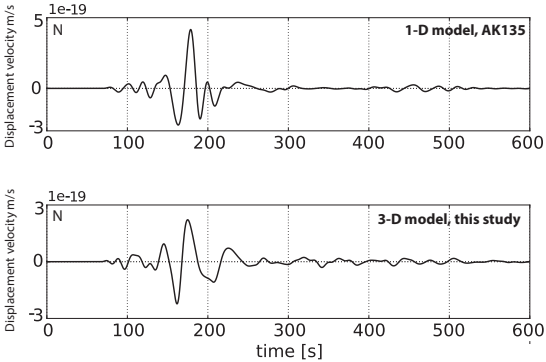

[Kennett et al., 1995]

Motivation

Green's functions for the same source-receiver path computed for 1-D (top) and 3-D (bottom) models clearly differ. If we were to use these 1-D Green's functions in the source inversion – all of this waveform difference would be incorrectly attributed to the source, while it is actually a structural effect.

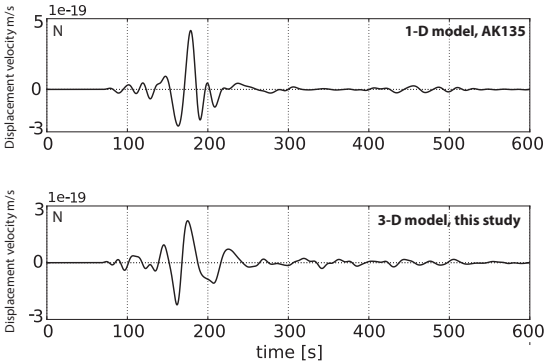

[Kennett et al., 1995]

- Incorrect Earth structure maps into and pollutes the source solution.

- We aim to account for the 3-D Earth structure and use this 3-D model to infer source parameters.

Forward modelling

In the following 3 slides, I will present our 3-D Earth model and show an example of the improved waveform fit. I will briefly introduce the Green's strain database and the theory behind it.

3-D Earth model for the Japanese Islands

Here you see a setup of the tomographic model which we constructed to be used for the source inversion.

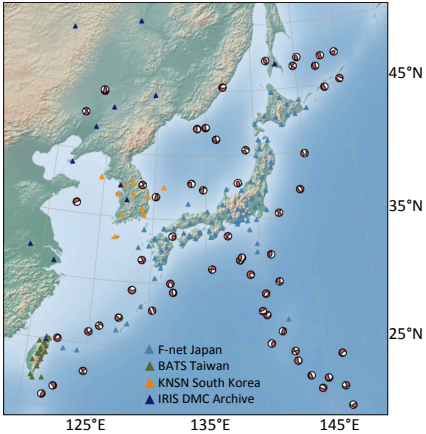

[Simutė et al., 2016]

Data

- 58 earthquakes (M_w 5 – M_w 7), 165 broadband stations
- *full waveforms:* body waves, surface waves
- period range: 15–80 s

Forward modelling

- SES3D wave propagation code, based on spectral-element method [Gokhberg & Fichtner, 2016]
- visco-elastic, anisotropic

Inverse modelling

- sensitivity kernels computed using adjoint methods

Constructed S-velocity model and improved waveform fit

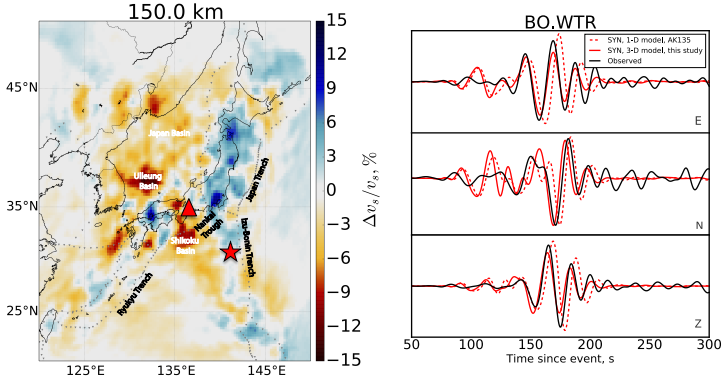

Left: depth slice of the isotropic S velocity perturbation of the tomographic model constructed for this study. **Right:** *observed data* vs synthetic data computed for a *1-D* AK135 model and synthetic data computed for a *3-D* model, constructed for this study for period range of 15–80 s for a M_w 5.2 event southeast of Honshu, at $\sim$ 50 km depth (red star on the map) and WTR station (red triangle on the map).

Database of Green's strains

In a point source configuration with any associated moment tensor **M**, one can easily compute displacement **u** if an easy access to the spatial gradient of Green's tensor $G_{in,q}$ is ensured:

$$u_i = M_{nq} * G_{in,q}$$

But computing $G_{in,q}$ for any potential source location is computationally prohibitive.

To alleviate the costs, we use reciprocity and compute receiver-side Green's strains. In turn, computational costs scale with the number of stations and is independent of the source area size.

We pre-compute and store Green's strains for a source area of interest.

The above expression can be further simplified assuming instantaneous source hypothesis, which is valid when the analyzed periods are much longer than the earthquake duration.

[Aki & Richards 2002]

Setup for the source inversion

We store the full wavefield in the source area of interest from the surface to 100 km depth (grey) for each station on the map. We compute synthetic displacement using these pre-computed Green's strains.

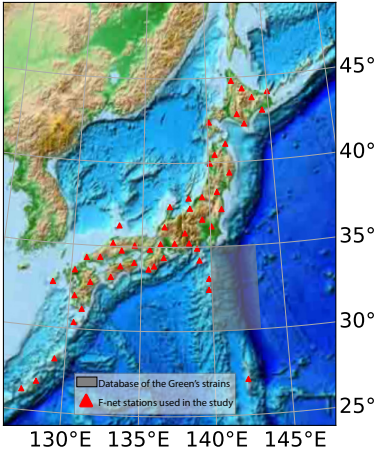

Data

- 3-component recordings, 52 F-net stations
- period range: 15–80 s

Synthetic data

- Computed from the Green's strain database

Misfit and model parameters of the source inversion

- *L2* norm, weighted windows
- 6 independent moment tensor components, 3 location parameters and a centroid time

Source inversion machinery

Here comes the inversion part. I introduce Hamiltonian Monte Carlo. For the inversion we use $15 - 80$ s data, $L2$ norm on weighted measurement windows and invert for 10 model parameters: 6 moment tensor components, 3 location parameters and the centroid time. Global CMT solution is used as a prior mean, as it provides a relatively good fit already.

Hamiltonian Monte Carlo

- HMC exploits derivative information of the misfit with respect to the inversion parameters in order to draw more plausible samples.
- As a result the sampling trajectory stays within the typical set and converges faster than derivative-free Monte Carlo methods.

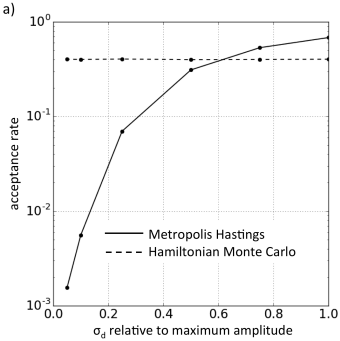

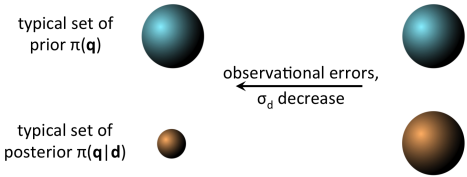

[Neal 2011, Betancourt 2017, Fichtner & Simutė 2018]

Moment tensor ensemble and relocation for a maximum likelihood model for 3 $\sim M_w 5$ events

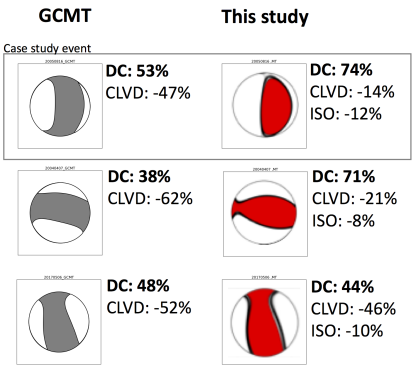

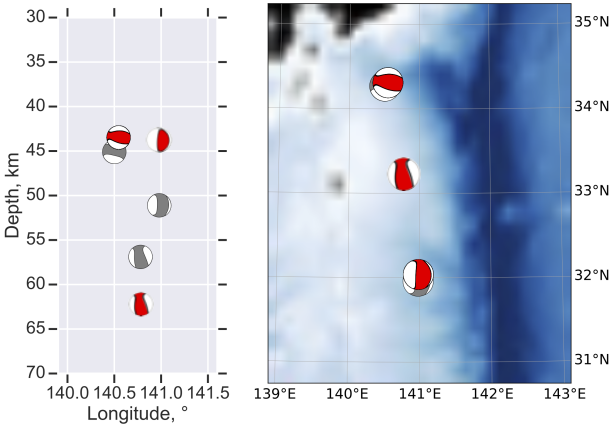

3-D Green's functions at short periods (15 – 80 s) allow for a larger DC component in the source solutions.

Probability density functions for a case study event

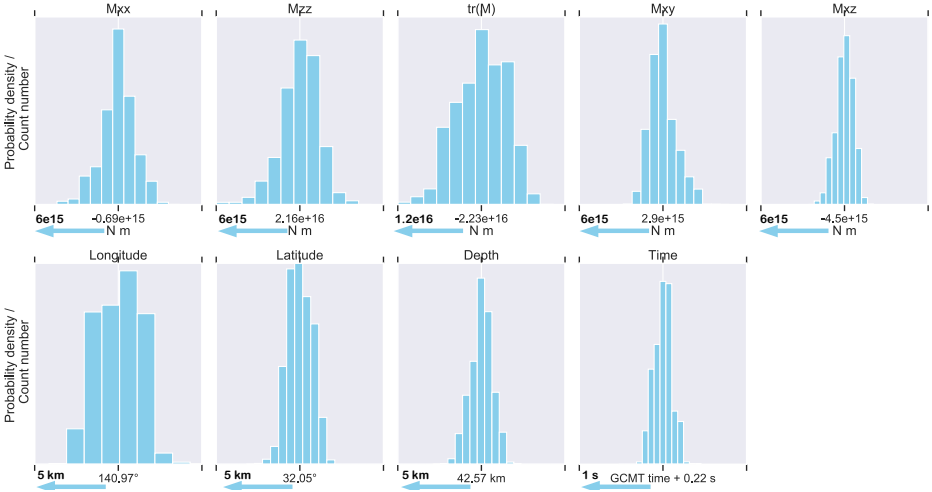

Isotropic components are more difficult to constrain, especially M_{zz}, as discussed by [Dufumier & Rivera 1997, Fitch et al., 1981].

Waveform fit for a case study event

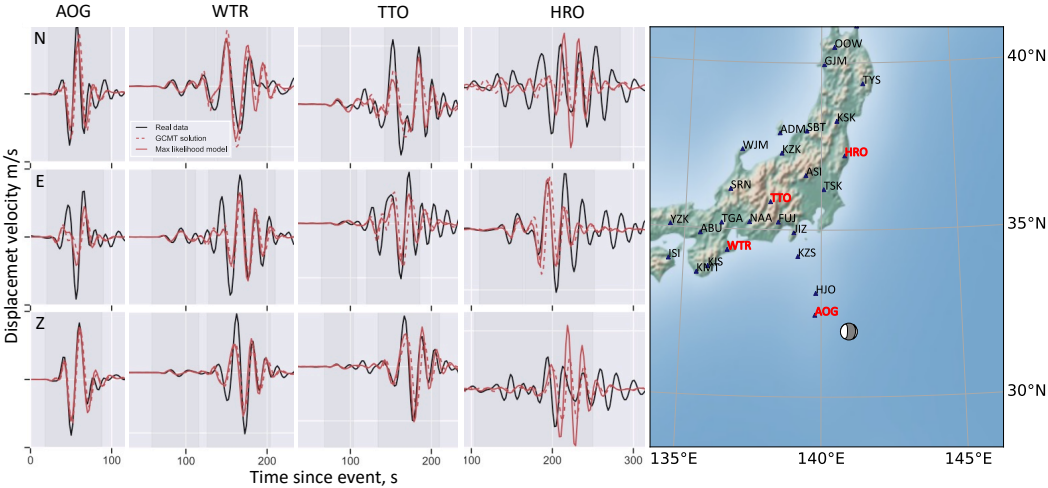

The fit improves on average by several percent across the traces compared to GCMT solution.

Results with isotropic component constrained to zero

GCMT

DC: 53%
CLVD: -47%

DC: 38%
CLVD: -62%

DC: 48%
CLVD: -52%

This study

DC: 74%
CLVD: -14%
ISO: -12%

DC: 71%
CLVD: -21%
ISO: -8%

DC: 44%
CLVD: -46%
ISO: -10%

This study, ISO=0

DC: 89%
CLVD: 11%

DC: 86%
CLVD: -14%

DC: 56%
CLVD: -44%

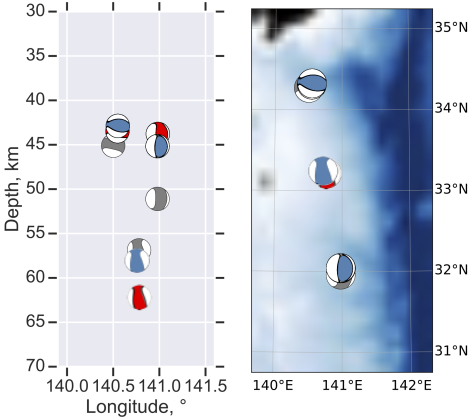

Constraining isotropic component allows for even larger DC component.

Summary

- Constructed a 3-D structural Earth model for the Japanese Islands
- Presented a workflow for a probabilistic source inversion in complex media
- Presented probabilistic inversion results for 3 $\sim M_w 5$ events in Izu Bonin region

Conclusions

- Data fit is (slightly) improved compared to the GCMT for 15–80 s data
- DC component tends to increase compared to GCMT, especially if the isotropic component is constrained to zero
- Taking into account a 3-D Earth structure allows for more tectonic-like event solutions

Summary

- Constructed a 3-D structural Earth model for the Japanese Islands
- Presented a workflow for a probabilistic source inversion in complex media
- Presented probabilistic inversion results for 3 $\sim M_w 5$ events in Izu Bonin region

Conclusions

- Data fit is (slightly) improved compared to the GCMT for 15–80 s data
- DC component tends to increase compared to GCMT, especially if the isotropic component is constrained to zero
- Taking into account a 3-D Earth structure allows for more tectonic-like event solutions

Thank you for reading!

References

- Kennett, B. L. N., Engdahl, E. R., and Buland, R. (1995) Constraints on seismic velocities in the Earth from traveltimes. *Geophys, J. Int.* 122, 108 – 124.
- Simutė, S., Steptoe, H., Gokhberg, A., and Fichtner, A. (2016) Full-waveform inversion of the Japanese islands region. *J. Geophys. Res.* 121, 3722 – 3741.
- Gokhberg, A. and Fichtner, A. (2016) Full-waveform inversion on heterogeneous HPC systems. *Comp. Geosci.* 89, 260 – 268.
- Dufumier, H. and Rivera, L. (1997) On the resolution of the isotropic component in moment tensor inversion. *Geophys, J. Int.* 131, 595 – 606.
- Fitch, Thomas J. and North, Robert G. and Shields, Michael W. (1981) Focal depths and moment tensor representations of shallow earthquakes associated with the Great Sumba Earthquake. *J. Geophys. Res.* 86(B10), 9357 – 9374.
- Aki, K. and Richards, P. (2002) *Quantitative Seismology*. University Science Books.
- Fichtner, A. and Simutė, S. (2018) Hamiltonian Monte Carlo inversion of seismic sources in complex media. *J. Geophys. Res.* 123, doi:10.1002/2017JB015249.
- Neal, R. M. (2011) MCMC using Hamiltonian dynamics. *Handbook of Markov Chain Monte Carlo*, ch. 5.
- Betancourt, M. (2017) A conceptual introduction to Hamiltonian Monte Carlo. *arXiv:1701.02434 [stat.ME]*.